

1 **Thresholds of fire response to moisture and fuel load differ between tropical savannas**
2 **and grasslands across continents**

3

4 Swanni T. Alvarado, Niels Andela, Thiago S. F. Silva, Sally Archibald

5

6 **Short running title:** Tropical savanna climate-fire responses

7

8 **Abstract**

9 **Aim:** An emerging framework for tropical ecosystems states that fire activity is either '*fuel*
10 *build-up limited*' or '*fuel moisture limited*' i.e. as you move up along rainfall gradients, the
11 major control on fire occurrence switches from being the amount of fuel, to the moisture
12 content of the fuel. Here we used remotely sensed datasets to assess whether interannual
13 variability of burned area is better explained by annual rainfall totals driving fuel build-up, or
14 by dry season rainfall driving fuel moisture.

15 **Location:** Pantropical savannas and grasslands

16 **Time period:** 2002-2016

17 **Methods:** We explored the response of annual burned area to interannual variability in
18 rainfall. We compared several linear models to understand how *fuel moisture* and *fuel build-*
19 *up effect* (accumulated rainfall during 6 and 24 months prior to the end of the burning season
20 respectively) determine the interannual variability of burned area and explore if tree cover,
21 dry season duration and human activity modified these relationships.

22 **Results:** Fuel and moisture controls on fire occurrence in tropical savannas varied across
23 continents. Only 24% of South American savannas were *fuel build-up limited* against 61% of
24 Australian savannas and 47% of African savannas. On average, South America switched from
25 fuel limited to moisture limited at 500 mm yr⁻¹, Africa at 800 mm yr⁻¹ and Australia at 1000
26 mm yr⁻¹ of mean annual rainfall.

27 **Main conclusions:** In 42% of tropical savannas (accounting for 41% of current area burned)
28 increased drought and higher temperatures will not increase fire, but there are savannas,
29 particularly in South America, that are likely to become more flammable with increasing
30 temperatures. These findings highlight that we cannot transfer knowledge of fire responses to
31 global change across ecosystems/regions – local solutions to local fire management issues are
32 required, and different tropical savanna regions may show contrasting responses to the same
33 drivers of global change.

34 **Keywords:** tropical savannas, fire regimes, fuel build-up, fuel moisture, ecosystem models,
35 future scenarios

36 1. Introduction

37 Understanding global controls on fire activity has become increasingly important in the
38 context of ecosystem drying and climatic change (Jolly *et al.*, 2015). In some ecosystems
39 drought events and rising temperatures may exacerbate fire risk (Bowman *et al.*, 2011; Price
40 *et al.*, 2015), and increase the incidence of large wildfires and fire-associated CO₂ emissions
41 (Voulgarakis & Field, 2015; Hantson *et al.*, 2017). However, not all ecosystems burn more
42 when exposed to drought and high temperatures. Pausas and Ribeiro (2013) showed that fire
43 in lower-productivity systems was unresponsive to temperature, and paleo-records highlight
44 regional differences in fire responses to changes in rainfall and temperature (Daniau *et al.*,
45 2012). Bradstock (2010) indicated that fire would respond to the factor that was most limiting
46 in a particular ecosystem – and when there is no fuel to burn increased temperatures and
47 drought conditions would be expected to have little impact on fire. Fires are therefore the
48 outcome of complex interactions between climate, fire, vegetation and land management
49 (Moritz *et al.*, 2012; Andela *et al.*, 2017; Forkel *et al.*, 2017; Abatzoglou *et al.*, 2018). Fire
50 enabled Dynamic Global Vegetation Models (DGVMs) are designed to model these
51 interactions, but model outcomes vary widely across models (Bowman *et al.*, 2014; Williams
52 & Abatzoglou, 2016; van Marle *et al.*, 2017), based on a wide range of different
53 parameterizations (Hantson *et al.*, 2016; Rabin *et al.*, 2017). The role of fire for carbon
54 cycling and maintaining biodiversity under scenarios of future change therefore remain
55 uncertain for tropical biomes.

56 Fire is an essential ecosystem process in tropical savannas and grasslands, which are
57 characterized by high fire frequency under natural conditions (Bond *et al.*, 2005; Chuvieco *et al.*,
58 2008). Rainfall is the dominant control on fire activity in the tropics (van der Werf *et al.*,
59 2008); seasonal variation in tropical savanna rainfall typically results in vegetation production
60 and biomass build-up during the wet season, followed by a dry period when dead or dormant
61 herbaceous vegetation becomes flammable (Bradstock, 2010). The dynamic balance of
62 productivity and seasonal drought also determines the interannual variability of burned area
63 (Pausas & Ribeiro, 2013). In the humid tropics fire activity is constrained by fuel moisture
64 conditions (*fuel moisture limited*) (Bradstock, 2010; Whitlock *et al.*, 2010): here negative
65 rainfall anomalies increase fire activity by causing usually green, non-flammable vegetation
66 to dry out sufficiently to carry fire (Aragão *et al.*, 2008). In contrast, in tropical biomes with
67 low net primary productivity such as grasslands and xeric savannas, fire activity is
68 constrained by fuel produced during the preceding growing seasons (*fuel build-up limited*)

69 (Whitlock *et al.*, 2010; O'Donnell *et al.*, 2011; Kahi & Hanan, 2018): here anomalous wet
70 years increase vegetation productivity which increases fire activity during the following dry
71 seasons (Van Wilgen *et al.*, 2004; Archibald *et al.*, 2010; Pausas & Paula, 2012; Abatzoglou
72 *et al.*, 2018).

73 Despite the important differences in fire ecology and behavior across fuel and moisture
74 limited fire regimes, their global distribution remains unknown. While climate determines
75 where and when fires can occur (van der Werf *et al.*, 2008; Archibald *et al.*, 2010), human
76 land management modifies regional patterns of fire activity (Bistinas *et al.*, 2013; Andela *et al.*,
77 2017). Humans are a source of ignitions as fire is often used as a tool in pastoral and
78 agricultural activities (Mistry, 2000; Cochrane & Ryan, 2009), but humans also alter fire sizes
79 by increasing landscape fragmentation and changing the timing of ignitions (Le Page *et al.*,
80 2010). Moreover, there is evidence that the sensitivity of fire regimes to climate variability
81 depends on human activities (Archibald *et al.*, 2010), as humans can “buffer” ecosystems
82 (Bird *et al.*, 2012) from climate and fire extremes through the way that they manage
83 landscapes and light fires (Yibarbuk *et al.*, 2002; Price *et al.*, 2012; Bird *et al.*, 2016).
84 Vegetation cover and type also interact with fire, as grasses produce fine fuels that carry
85 savanna fires. Tree cover in turn, may reduce fire occurrence by limiting grass productivity
86 (Bond *et al.*, 2005; Hoffmann *et al.*, 2012; Aleman & Staver, 2018). The effects of climate
87 and human land management on fire activity are therefore further modified by vegetation
88 type, its cover and productivity (Archibald *et al.*, 2009; Bistinas *et al.*, 2014; Lehmann *et al.*,
89 2014).

90 Here we use satellite observations to study burned area-rainfall relationships across a
91 moisture gradient, ranging from xeric grasslands to mesic tropical savannas. First, we identify
92 pantropical rainfall thresholds where savanna and grassland fire regimes switch from *fuel*
93 *build-up limited* to *fuel moisture limited*. Second, we investigate how these thresholds vary
94 across regions and how spatial patterns in *fuel build-up-* and *fuel moisture limited* fire regimes
95 are modified by rainfall seasonality, human activity, and tree cover. Understanding how
96 climate, human activity, and ecosystem structure modify the response of fire activity to
97 changing weather conditions is critical to model and forecast future fire activity across
98 different environments.

99 **2. Data and methods**

100 **2.1. Remote sensing data**

101 For our analysis, we rescaled all data to 0.25° spatial resolution by calculating the mean value,
102 land cover type formed a notable exception as we used the dominant cover type within each
103 larger 0.25° grid cell.

104 **Savanna and grassland cover.** We used the Moderate Resolution Imaging
105 Spectroradiometer (MODIS) Global Land Cover product (MCD12C1 collection 5.1) for 2012
106 (Friedl *et al.*, 2010) to delimit savanna and grassland extent across continents. We included all
107 0.25° grid cells (25°N - 25°S) where savannas and grasslands formed the dominant land cover
108 type, based on the combined cover of “woody savannas”, “savannas”, and “grasslands”
109 according to the International Geosphere-Biosphere Programme (IGBP) classification. We
110 focus on “natural lands”, by excluding croplands and urban areas from our analysis, because
111 we expect that fuel-build up and moisture status would primarily depend on management
112 practice instead of antecedent rainfall across these landscapes. In addition, we used the
113 MODIS vegetation continuous fields product (MOD44B collection 5 for 2010, (DiMiceli *et*
114 *al.*, 2011) to exclude areas with tree cover > 40%, assuming that savannas with high tree
115 cover are less flammable (Archibald *et al.*, 2009), and because fires are difficult to detect
116 under canopies (Morton *et al.*, 2011). In this study we analyzed data from Africa (55.6%),
117 Australia (7.8%) and South America (27.4%), together containing 90.8% of the delimited
118 tropical savannas and grasslands. Tropical savannas in Asia (6.1%) and Central America
119 (3.1%) are highly fragmented and poorly defined (e.g., Ratnam *et al.*, 2016), and were
120 therefore excluded from our analysis.

121 **Burned area data.** We derived the percentage of monthly burned area per 0.25° grid cell
122 from the MODIS MCD64A1 collection 6 global burned area product (Giglio *et al.*, 2018).
123 Subsequently, we derived time series of annual burned area (BA in % yr⁻¹) per fire year for
124 each 0.25° grid cell for 2002–2016. For each grid cell, we delimited the fire-year as the 12-
125 month period centered on the month of maximum mean burned area (from 5 months before to
126 6 months after the month of maximum burned area). This step is required because in the
127 northern hemisphere tropics the fire season typically includes months of two calendar years,
128 with maximum fire activity occurring in December or January. Based on these fire years, we
129 defined the start and end months of the burning season as the all-year mean month where 10%
130 and 90% of annual burned area had occurred, respectively. Our analysis is based on the
131 assumption of clear seasonality with a unique fire season per year, which is generally true
132 across tropical grasslands and savannas (Benali *et al.*, 2017).

133 **Burned area drivers.** Monthly rainfall data were obtained from the Climate Hazards Group
134 InfraRed Precipitation with Station (CHIRPS) dataset (Funk *et al.*, 2015) for the extended
135 study period between 2002–2016. We used rainfall data to calculate mean annual rainfall
136 (MAR, in mm yr⁻¹, Fig 1b) over the calendar year and estimate the *fuel moisture* and *fuel*
137 *build-up effects* on interannual variability in burned area. We defined the *fuel moisture effect*
138 as the accumulated rainfall during the six months prior to the end of the burning season. We
139 assumed that rainfall occurring during, or just before the burning season determines the
140 probability of ignition and fire spread. The *fuel build-up effect* was defined as the accumulated
141 rainfall during 24 months prior to the end of the burning season, as previous rainfall is an
142 important control on the amount of biomass produced. We selected the 6- and 24-months cut-
143 off as, on average, the strongest negative response in *fuel moisture limited* landscapes was
144 found around 6-7 months of antecedent rainfall (Fig. A1), while across *fuel build-up limited*
145 landscapes accumulated rainfall over two wet seasons (24-months) had a slightly higher
146 explanatory power than over a single wet season (12-months) (Fig. A1).

147 We considered three explanatory variables for our initial analysis of the drivers of
148 observed spatial patterns in *fuel build-up* and *fuel moisture limited* fire regimes. First, we
149 focus on spatial differences in dry season duration. Following Hulme & Viner (1998), we
150 define the dry season duration (in months) as the average number of months with rainfall
151 below 50 mm month⁻¹ during the 2002 – 2016 calendar years (Fig. A2b). This intermediate
152 (50 mm month⁻¹) rainfall threshold assures reasonable sensitivity to dry season duration
153 across both arid and more humid tropical environments. Second, to investigate how humans
154 affect fire occurrence and climate-fire interactions, we used the Wildlife and Conservation
155 Society (WCS) Human Influence Index (HII, Fig. A2a) (WCS & University, 2005), a
156 measure, varying between 0 and 64 (for no human and maximum influence respectively), of
157 the direct human influence on ecosystems based on eight different measures of human
158 presence: population density (people per km²), land cover type, and a measure of the presence
159 of railroads, major roads, navigable rivers, coastlines, nighttime stable lights, and urban
160 polygons. Third, because vegetation structure can affect fire activity and varies across
161 continents (Lasslop *et al.*, 2018), we also considered tree cover as an explanatory variable for
162 observed patterns of *fuel* and *moisture limited* fire regimes. Tree cover data was obtained from
163 MODIS vegetation continuous fields (MOD44B collection 5, Fig. A2c) for 2010 (DiMiceli *et*
164 *al.*, 2011). Because in our definition of tropical savannas and grasslands we already excluded
165 areas with tree cover >40%, this variable ranged from 0 to 40%.

166 **2.2. Methods**

167 **Burned area response to *fuel moisture* and *fuel build-up* effects.** Based on the per-fire-year
168 burned area time series, we explored the response of annual burned area to interannual
169 variability in rainfall for each 0.25° grid cell. All grid cells that showed negative correlations
170 (Pearson's r) between antecedent rainfall accumulated over 6 months prior to the end of the
171 burning season and annual BA were considered *fuel moisture limited* fire regimes, indicating
172 higher burned area when accumulated rainfall was low during or shortly before the burning
173 season. Similarly, we considered ecosystems to be *fuel build-up limited*, for all grid cells with
174 a positive correlation between annual BA and antecedent rainfall accumulated during 24
175 months prior to the end of the burning season. Some grid cells had both negative correlations
176 (*fuel moisture effect*) with the short lead times and positive correlations (*fuel build-up effect*)
177 with the long lead times, but in these cases, effects were generally not significant at the same
178 time ($p < 0.05$ in 5% of total grid cells). For simplicity, we therefore selected the strongest
179 absolute correlation for each grid cell.

180 Based on the biome wide characterization of burned area response to antecedent rainfall,
181 we explored how these relationships varied across continents. First, we identified the MAR
182 threshold where fire regimes switched from being *fuel build-up limited* to being *fuel moisture*
183 *limited*. We binned the per grid cell strongest absolute (i.e. positive or negative) correlation
184 between annual BA and antecedent rainfall into 100 mm MAR bins. We then defined the
185 threshold where ecosystems switched from *fuel build-up limited* to *fuel moisture limited* (and
186 vice versa) as the MAR bin where >50% of the correlation coefficients switched from
187 negative to positive (i.e. the median value in a boxplot crossed the zero line).

188 **Drivers of burned area response.** We used two different approaches to explore the drivers
189 of spatial differences in the relationship between annual burned area and antecedent rainfall.
190 First, to keep annual rainfall constant, we binned all grid cells based on 200 mm yr⁻¹ MAR
191 increments; within each rainfall bin, we further subdivided the grid cells based on bins of dry
192 season duration (DS; increments of months with rainfall below 50 mm), Human Influence
193 Index (HII; increments of 5 units of HII, HII ranged from 0 to 40 across the study area), and
194 tree cover (TC; 5% increments from 0 to 40%). Based on this subdivision along rainfall
195 gradients, we explored how DS, HII, and TC modified patterns of a) mean annual burned
196 area, b) interannual variability in burned area (measured as the coefficient of variation), and c)
197 the correlation coefficient between antecedent rainfall and annual BA.

198 Second, we compared two multiple linear regression models to understand how the *fuel*
199 *moisture effect* (Rain6, 6 months of accumulated rainfall) and the *fuel build-up effect* (Rain24,
200 24 months of accumulated rainfall) influenced the interannual variability of BA (Eq. 1) and
201 investigate if BA response to rainfall varied at continental scales (Eq. 2). In order to increase
202 model sensitivity to temporal variability in burned area, we used burned area anomalies rather
203 than absolute burned area time series.

204

$$205 \quad \text{BA}_{i,j} \text{ anomaly} \sim \alpha + \beta_1 * \text{Rain6}_{i,j} + \beta_2 * \text{Rain24}_{i,j} + \varepsilon \quad \text{Equation 1}$$

$$206 \quad \text{BA}_{i,j} \text{ anomaly} \sim \alpha + \beta_1 * \text{Rain6}_{i,j} : \text{Continent} + \beta_2 * \text{Rain24}_{i,j,t} : \text{Continent} + \varepsilon \quad \text{Equation 2}$$

207 where $\text{BA}_{i,j}$ anomaly is the burned area anomaly for each pixel (i) and year (j) calculated as
208 $\text{BA}_{i,j} - \text{mean BA}_i$, β parameters represent the slope of the linear regression between the BA
209 anomaly and the explanatory variables (Rain6_{i,j} and Rain24_{i,j,t}), α is the intercept and ε the
210 residual error term. The BA anomaly includes both negative and positive values, where
211 negative values indicate that the BA for the year *j* was lower than the mean BA and positive
212 values indicate that annual BA was higher than the mean. Thus, β_1 and β_2 indicate the rate of
213 BA change per unit of accumulated rainfall (% year⁻¹ mm⁻¹).

214 Next, we explored how other variables, including MAR, DS, HII and/or TC modify the
215 influence of antecedent rainfall on burned area anomalies by analyzing how the β_1 and β_2
216 values changed when introducing each driver in the model. In addition, when including a new
217 variable, we compared the model with and without the effect in question, using an ANOVA
218 likelihood-ratio test and AIC (Akaike's Information Criterion) to confirm the selection of the
219 best model (Burnham & Anderson, 2004). Finally, we constructed the same models, but now
220 based on full burned area time series instead of anomalies. This analysis helped to understand
221 how each variable contributes to both spatial and temporal patterns of biome wide burned
222 area. All analyses were done using the 'raster' and 'rgdal' packages in R, version R2.5.1 (R
223 Core Team, 2016).

224 **3. Results**

225 **3.1. Burned area response to antecedent rainfall**

226 We observed the strongest correlations between antecedent rainfall and annual burned area
227 (BA) in frequently burning savannas and grasslands across the tropics (Fig. 1). Here we
228 considered grid cells with a negative correlation between burned area and rainfall (6-month
229 lead time) to be *fuel moisture limited* and grid cells with a positive correlation (24-month lead

230 time) to be *fuel build-up limited*. Interestingly, we found that savannas with *fuel build-up*
231 *limited* fire regimes (41.4%) in more arid regions covered less area than savannas with *fuel*
232 *moisture limited* fire regimes (58.6%, Fig. 1b, e) in more humid systems. Mean annual rainfall
233 (MAR) varied widely across tropical savannas on the three continents, resulting in
234 predominantly *fuel moisture limited* fire regimes across the relatively humid savannas of
235 South America, and *fuel build-up limited* fire regimes across Australian savannas that were
236 more arid on average (Fig. 1b to 1e). Africa showed a mix of *fuel* and *moisture limited*
237 savannas across a large rainfall gradient. For example, we observed strong positive
238 correlations for arid regions (e.g. Namibia, Botswana and Zimbabwe) and strong negative
239 correlations for humid regions (e.g. the north of Mozambique and the south of Tanzania and
240 the Democratic Republic of Congo) (Fig. 1e).

241 **3.2. Continental differences in the switch from fuel build-up to fuel moisture** 242 **limitation**

243 Africa tropical savanna and grassland fire regimes switched from a predominantly positive
244 (*fuel build-up effect*) to negative (*fuel moisture effect*) response to antecedent rainfall around
245 800 mm annual rainfall (Fig. 2), while fire regimes in South America switched around 500
246 mm yr⁻¹, and in Australia around 1000 mm yr⁻¹ (Fig. 2). For all three continents, MAR bins
247 that contained a low number of grid cells often showed a more variable response (cf. Figs. 2
248 and A3). We also observed large spatial variability in burned area-rainfall responses (Fig. 1
249 and 2), indicating that the switch from *fuel build-up* to *fuel moisture limited* fire regimes
250 occurred gradually. On each continent, there was a transition zone in MAR levels rather than
251 a clear threshold, where the strength of the dominant correlation weakened before switching
252 to a different dominant driver. Only 24% of South American savannas were *fuel build-up*
253 *limited* against 61% of Australian savannas and 47% of African savannas.

254 **3.3. Drivers of continental differences.**

255 In addition to MAR, we explored how rainfall seasonality influences median annual BA
256 and interannual variability in BA, both important indicators of the strength of fire-climate
257 interactions. Globally, longer dry season durations tended to increase median annual BA,
258 particularly in intermediate productive savannas and grasslands (MAR between 900-1500
259 mm, Fig 3a). Interestingly, when dry season length exceeded 9 months, annual burned area
260 typically declined again, likely because very short growing seasons may limit ecosystem
261 productivity and thus fuel availability. In addition to burned area, we also analyzed its
262 coefficient of variation, we hypothesize that the strength of the burned area response to

263 antecedent rainfall partly depends on the variability of both variables. For bins of comparable
264 rainfall and dry season duration, Australia showed the lowest coefficients of variation,
265 potentially weakening correlation coefficients between antecedent rainfall and burned area,
266 seen as a more variable response of positive and negative correlations (Fig 3b and c). In
267 contrast, large on average coefficients of variation across South America may be responsible
268 for the relatively strong negative correlation observed across productive savannas. We also
269 observed a reduction in the coefficient of variation in areas of high fraction of annual burned
270 area (Fig. 3b), possibly reducing the strength of the correlation between annual burned area
271 and fuel conditions (Fig. 3c). Although dry season duration clearly affected burned area and
272 its variability, patterns were not uniform, suggesting other factors also played a role.

273 Human impact strongly reduced burned area across continents (Fig. 4a), while Australian
274 savannas and grasslands were generally characterized by low human impact values (HII <10)
275 and African and South American savannas were characterized by higher impact values (HII =
276 10-25; Fig. 4b). The coefficient of variation was clearly reduced in natural areas with a large
277 fraction of burned area and low human influence (Fig. 4b). Despite the large impact of HII on
278 absolute burned area, impacts on the interannual variability were more limited and complex.
279 Globally, a small decline in the strength of the burned area response to rainfall variability was
280 observed with decreasing HII and increasing burned area in the peak biomass burning regions
281 (MAR ranging from 900 – 1500 mm yr⁻¹; Fig. 4c). In contrast, at continental scales sometimes
282 the opposite pattern was observed. For example, in productive savannas (MAR 1300 – 2100
283 mm yr⁻¹) of South America the negative correlation between antecedent rainfall and burned
284 area strengthened with decreasing HII. The global pattern in the response of BA to the *fuel*
285 *build-up* and *fuel moisture effects* was mainly determined by South America and Africa, with
286 a dominant negative response in savannas with MAR above 900 mm yr⁻¹ and positive
287 response in savannas with MAR below 900 mm yr⁻¹, independently of the HII (Fig. 4c).

288 Vegetation structure also influenced biome wide patterns of burned area and the strength
289 and sign of correlation coefficients between antecedent rainfall and burned area (Fig. 5). As
290 expected, we observed that higher tree cover was often associated with reduced burned area,
291 particularly in the humid tropics (Fig. 5a). In productive savannas (MAR ranging from 900 to
292 2000 mm yr⁻¹), the fuel moisture effect tended to strengthen with increasing tree cover,
293 although relationships were often weak (Fig. 5c). In fuel limited ecosystems of Australia,
294 there was a weak increase in the strength of the fuel build-up effect with tree cover, opposite
295 to the global pattern, where the strength of the fuel build-up effect weakened with increasing

296 tree cover. As noted earlier, coefficients of variation varied widely across continents, possibly
297 strengthening or weakening regional correlation coefficients. In contrast to Africa and
298 Australia, South America showed high coefficients of variation for savannas of intermediate
299 productivity, likely contributing to the exceptionally strong moisture limitation on regional
300 burned area.

301 Despite the clear biome wide patterns of *fuel moisture* and *fuel build-up limited* fire
302 regimes, we could not establish a single global model to explain the interannual variability in
303 burned area (BA) based on *fuel build-up effect* and *fuel moisture effect* alone (Table 1). Here
304 we used multiple linear regression models to test the effect of the antecedent rainfall on BA
305 anomalies (Table 1) per pixel across the time series, and the spatial and temporal pattern in
306 BA time series (Table A1), across tropical savannas and grasslands. We expect that the model
307 based on BA anomalies is better able to capture interannual variability, while the second
308 model captures both temporal variability and spatial patterns of burned area. The global
309 model of BA anomalies that included only the *fuel build-up effect* and *fuel moisture effect* as
310 explanatory variables explained less than 1% of BA variation (Table 1), while the same model
311 for absolute BA explained 3% of the variance (Table A1). Surprisingly, BA did not vary as
312 expected when an interaction term between MAR and *fuel build-up effect* and *fuel moisture*
313 *effect* was added to the model and its performance did not improve. In contrast, the inclusion
314 of “continent” as an interaction term with the 6- and 24-month accumulated rainfall increased
315 the percent of explained variance and reduced AIC for both BA (from 3.6 to 19%, Table A1)
316 and its interannual variability (from 0.0019 to 0.0029%, Table 1). Both models, supported
317 different slopes between the *fuel moisture effect* and *fuel build-up effect* and burned area
318 across continents ($p < 0.001$), confirming continental scale differences in burned area-rainfall
319 response (Table 1 and A1, Fig. 2).

320 The models with the highest explanatory power (lowest AIC) explained 0.4% of the
321 variance of the interannual variability of BA (Table 1) and 29% of spatial occurrence (Table
322 A1). These models included *tree cover*, *dry season duration* and *HII* all in interaction with
323 *Continent* as additional factors to *fuel build-up effect* and *fuel moisture effect*. The response of
324 BA anomalies to the *fuel-moisture effect* and the *fuel build-up effect* was strongest in Australia
325 ($\beta_1 = -0.0036 \text{ \% mm}^{-1}$ and $\beta_2 = 0.0019 \text{ \% mm}^{-1}$ respectively, Table 1) and weakest in Africa
326 ($\beta_1 = -0.0012 \text{ \% mm}^{-1}$ and $\beta_2 = 0.00035 \text{ \% mm}^{-1}$ respectively, Table 1). Statistical analysis
327 confirmed the expected response, with negative slope coefficients for *fuel moisture effect* and
328 positive coefficients for *fuel build-up effect* (Table 1). The inclusion of *tree cover*, *dry season*

329 *duration* or *HII* in the models modified the slopes of *fuel build-up effect* across all the three
330 continents, while the slopes for *fuel moisture effect* remained more similar (Table 1). When
331 we included all three variables in the model, we detected a slight decrease in the slope of *fuel*
332 *build-up effect* for African (from 0.00041 to 0.00035% mm⁻¹) and South America savannas
333 (from 0.00058 to 0.00046% mm⁻¹) and a larger increase for Australian savannas (from
334 0.00088 to 0.0019% mm⁻¹, Table 1). The inclusion of these three factors also modified the
335 intercept sign from negative to positive indicating a positive anomaly (BA > mean BA) when
336 these factors are zero. When considering the inclusion of each of these explanatory variables
337 (DS, HII, and TC) separately, the inclusion of dry seasons length had the strongest effect on
338 the response of BA to the *fuel build-up effect*; in Africa β_2 decreased from 0.00041 to
339 0.00023% mm⁻¹ and the smallest effect was observed in South America from 0.00058 to
340 0.00051 % mm⁻¹. In contrast, the inclusion of HII had the strongest effect on the response of
341 BA to the *fuel build-up effect* in Australia β_2 , increasing from 0.00088 to 0.0011% mm⁻¹ while
342 in Africa and South America we observed a slight decrease (from 0.00041 to 0.00040% mm⁻¹
343 and from 0.00058 to 0.00054% mm⁻¹ respectively). The inclusion of tree cover had the
344 strongest effect on the response of BA to the *fuel build-up effect* for South America, β_2
345 increased from 0.00058 to 0.010% mm⁻¹. When we analyzed the absolute BA (Table A1), HII
346 coefficients were also negative for the three continents, in line with lower burned area in
347 human dominated landscapes (Archibald *et al.*, 2012; Andela *et al.*, 2017), with the highest
348 decrease in BA variation when human influence increased in Australia ($\beta_4 = -3.10\%$), and a
349 similar lower variation observed in Africa and South America ($\beta_4 = -1.29\%$ and -1.10%
350 respectively, Table A1).

351

352 **4. Discussion**

353 **4.1. Fire-climate threshold**

354 Here we explore the extent of *fuel build-up* and *fuel moisture limited* fire regimes across
355 tropical savannas based on a per-pixel temporal correlation between burned area and
356 antecedent rainfall. Savanna fire-climate interactions changed along gradients of mean annual
357 precipitation, with burned area in xeric savannas being primarily limited by fuel build-up and
358 in mesic savannas by fuel moisture (Fig. 1, Krawchuk & Moritz, 2011; Kahiu & Hanan,
359 2018). In line with previous work, we find that fire activity in humid savannas and grasslands
360 primarily responds to drought conditions during the fire season (Archibald *et al.*, 2010;
361 Lehsten *et al.*, 2010; Alvarado *et al.*, 2017) similar to tropical rainforests (Aragão *et al.*,

362 2008). We find that fuel moisture was the dominant control on fire activity over 58.6% of
363 tropical savannas and grasslands. These systems currently account for 59.1% of the tropical
364 area burned, and the remaining 40.9% is in systems are fuel build-up limited.

365 Striking differences were observed across continents, with large areas of *fuel build-up*
366 *limited* fire regimes occurring across more arid grasslands and savannas of southern Africa
367 and northern Australia, and a near-absence of *fuel build-up limited* systems in tropical South
368 America (Figs. 1 and 2). Fuel moisture formed the key control on burned area across South
369 America's savannas, except for more arid grasslands along the eastern edge of the Brazilian
370 Cerrado. Burned area in arid regions of Africa and Australia responded strongly to antecedent
371 rainfall, highlighting the importance of fuel build-up and connectivity in these regions
372 (Archibald *et al.*, 2010; Whitlock *et al.*, 2010; Krawchuk & Moritz, 2011; Price *et al.*, 2015).
373 Continental scale differences were partly driven by differences in climate, for example, the
374 extent of semi-arid and arid savannas with $MAR < 1000 \text{ mm yr}^{-1}$ was largest across Africa and
375 Australia, resulting in an overall larger fraction of ecosystems where fire occurrence was
376 limited by *fuel build-up* (Fig. 1; Archibald *et al.*, 2010a). However, savanna fire regimes also
377 switched from being dominantly *fuel build-up limited* to *fuel moisture limited* at different
378 thresholds, around 500 mm yr^{-1} in South America, 800 mm yr^{-1} in Africa, and 1000 mm yr^{-1}
379 in Australia (Fig. 2). Together, these two factors resulted in continental scale differences in
380 fire regimes, and fire activity was limited by *fuel build-up* in only 24% of South American
381 savannas, against 47% of African savannas and 61% of Australian savannas. Interestingly,
382 these continental differences in fire regimes are in line with previous work showing similar
383 differences in controls on savanna distribution and structure (Lehmann *et al.*, 2011, 2014). In
384 the transition zones, where fire regimes switched from being predominantly *fuel-build up*
385 *limited* to *fuel moisture limited*, the relationship between burned area and fuel dryness or fuel
386 availability was often weak, and likely further modified by other climatic, ecological, and
387 anthropogenic factors influencing fuel conditions.

388 **4.2. Drivers of fire response**

389 Seasonal rainfall distribution varied considerably across continents and had a strong effect on
390 annual burned area (Fig. 3a). Previous analyses have shown that rainfall amount during the
391 dry and wet seasons contribute to explain the spatial patterns of tropical fire activity (van der
392 Werf *et al.*, 2008; Bowman *et al.*, 2014; Chen *et al.*, 2017), and that climate seasonality can
393 explain observed differences in fire activity across regions with similar MAR (Saha *et al.*,
394 2019). We found that a minimum dry season duration of 6 to 8-months was required for

395 frequent fires to occur in productive and humid savannas, but we only detected a weak
396 relationship between annual burned area and increasing dry season lengths longer than six
397 months. A possible explanation for this weak relationship could be that dry season duration
398 longer than six months may limit herbaceous productivity by shortening the growing season
399 in spite of MAR. In addition, our results suggest that observed differences in rainfall
400 seasonality may also modify the response of burned area to antecedent rainfall across different
401 regions (Fig. 3b and c). Although the relatively long and pronounced African dry season is
402 one of the factors contributing to high fire frequencies across the continent (Archibald *et al.*,
403 2009), African savannas were characterized by relatively low variability in burned area. In
404 contrast, South American savannas were characterized by lower fire frequencies, but showed
405 higher interannual variability in burned area driven by climate anomalies (cf. Figs. 3b and c;
406 Alvarado *et al.*, 2017b; Chen *et al.*, 2017; Mataveli *et al.*, 2018).

407 Several analyses have shown that human land management, and therefore population
408 density has a significant impact on global burned area (Bistinas *et al.*, 2013). In line with
409 these findings, we found that higher human influence significantly reduced burned area across
410 continents, with larger consequences for more densely populated continents like Africa and
411 South America compared to Australia (Fig. 4a and Table A1; Archibald *et al.*, 2012; Andela
412 *et al.*, 2017). Previous work has also shown that human land management may reduce the
413 sensitivity of fire regimes to climate extremes (Bird *et al.*, 2016). We found that the observed
414 biogeographic differences in fire responses to antecedent rainfall could be related to human
415 land management to some extent, but this factor alone could not explain the differences
416 observed across continents (Fig. 4c). In general, areas with large annual mean burned area and
417 low population densities, showed a relatively strong burned area response to rainfall
418 variability. Nevertheless, this pattern did not hold everywhere, and particularly in savannas of
419 intermediate productivity we observed an overall increase in the strength of the fuel-moisture
420 effect on burned area in human dominated landscapes.

421 Continental scale differences in tree cover also explained part of the observed differences
422 in fire-climate interactions. Previous work has shown that tree cover may limit fire activity in
423 savannas (Archibald *et al.*, 2009), though these effects may be partly masked out in our study,
424 that focuses on more open cover types with tree cover smaller or equal to 40%. Across areas
425 with *fuel moisture limited* fire regimes, we observed a slight increase in the strength of the
426 responses of BA to the antecedent rainfall with the increase of tree cover at similar MAR.
427 While all three variables (DS, HII and TC) modified the response of burned area to antecedent

428 rainfall, none of these variables could explain the differences in thresholds observed across
429 the continents (Figs. 3, 4 and 5). For example, when controlling for TC, continental scale
430 differences in rainfall thresholds at which savannas switched from *fuel build-up* to *fuel*
431 *moisture limited* fire regimes remained different.

432 To confirm these findings, we used a range of multiple linear regression models to explore
433 if the continental scale differences could be explained by differences in DS, HII, and TC.
434 Allowing the burned area to respond differently to antecedent rainfall across continents
435 caused a considerable model improvement both when modeling absolute burned area (Table
436 A1) or it's variability (Table 1). While the introduction of DS, HII and TC as additional
437 explanatory variables further improved model performance, they only marginally affected
438 continental scale differences in burned area response to antecedent rainfall (compare slopes in
439 Table 1). Nevertheless, our linear model explained just 29% of absolute burned area and
440 about 1% of the burned area anomalies even when considering continental scale differences in
441 DS, HII and TC as additional drivers. Improving model representation of fire response to
442 antecedent rainfall therefore remains a topic of future investigation. While we explored the
443 role of dry season duration, it is possible that other indicators of vegetation and fuel
444 conditions, like evapotranspiration, also play an important role (Boer et al. 2016). Similarly,
445 regional differences in herbivory and human fire management, as well as the different
446 composition and structure of grass and tree communities across continents may also be
447 important (Lehmann et al., 2011).

448 Understanding the distribution of *fuel build-up* - and *fuel moisture limited* fire regimes is
449 critical for fire management now and in the future, as changes in land management or climate
450 may result in contrasting responses across *fuel* and *moisture limited* systems. In contrast to
451 earlier studies that have suggested that fire activity in savannas was mostly limited by fuel
452 availability (Whitlock *et al.*, 2010; Krawchuk & Moritz, 2011), we found that fuel moisture
453 controlled burned area variability in more than half (58.6%) of the tropical savannas and
454 grasslands, accounting for 59,1% of total burned area. Striking differences in burned area
455 response to rainfall variability across continents highlighted that South American savannas
456 were particularly sensitive to fuel moisture conditions, suggesting that rising temperatures
457 may increase fire activity across the continent, and explaining the extraordinary strong
458 response of fire activity across the continent to drought conditions driven by sea surface
459 temperature anomalies (Chen et al., 2011). In contrast, a reduction of moisture availability
460 would likely decrease burned area over most of Australia, where fire activity was mainly
461 controlled by fuel build-up. In African savannas and grasslands, the area where burned area

462 was primarily controlled by fuel build-up was about equal to the area where fuel moisture
463 conditions were most important. Although we could not conclusively attribute the continental
464 scale differences to a single driver, we found that rainfall seasonality, human land
465 management and tree cover all modified fire-climate interactions regionally through their
466 effects on fuel availability and moisture status. Our work demonstrates that one single “global
467 model” for savanna fires will not be enough to predict future fire regimes and fire regimes
468 across different continents will likely respond differently to the same drivers of global change.

469

470 **References**

- 471 Abatzoglou, J.T., Williams, A.P., Boschetti, L., Zubkova, M. & Kolden, C.A. (2018) Global patterns of
472 interannual climate–fire relationships. *Global Change Biology*, **24**, 5164–5175.
- 473 Aleman, J.C. & Staver, A.C. (2018) Spatial patterns in the global distributions of savanna and forest. *Global*
474 *Ecology and Biogeography*, **27**, 792–803.
- 475 Alvarado, S.T., Fornazari, T., Cóstola, A., Morellato, L.P.C. & Silva, T.S.F. (2017) Drivers of fire occurrence in
476 a mountainous Brazilian cerrado savanna: Tracking long-term fire regimes using remote sensing.
477 *Ecological Indicators*, **78**, 270–281.
- 478 Andela, N., Morton, D.C., Giglio, L., Chen, Y., van der Werf, G.R., Kasibhatla, P.S., DeFries, R.S., Collatz,
479 G.J., Hantson, S., Kloster, S., Bachelet, D., Forrest, M., Lasslop, G., Li, F., Mangeon, S., Melton, J.R.,
480 Yue, C. & Randerson, J.T. (2017) A human-driven decline in global burned area. *Science*, **356**, 1356–
481 1362.
- 482 Aragão, L.E.O.C., Malhi, Y., Barbier, N., Lima, A., Shimabukuro, Y., Anderson, L. & Saatchi, S. (2008)
483 Interactions between rainfall, deforestation and fires during recent years in the Brazilian Amazonia.
484 *Philosophical Transactions of the Royal Society B: Biological Sciences*, **363**, 1779–1785.
- 485 Archibald, S., Nickless, A., Govender, N., Scholes, R.J. & Lehsten, V. (2010) Climate and the inter-annual
486 variability of fire in southern Africa: a meta-analysis using long-term field data and satellite-derived burnt
487 area data. *Global Ecology and Biogeography*, **19**, 794–809.
- 488 Archibald, S., Roy, D.P.D., Wilgen, V., Brian, W. & Scholes, R.J. (2009) What limits fire? An examination of
489 drivers of burnt area in Southern Africa. *Global Change Biology*, **15**, 613–630.
- 490 Archibald, S., Staver, A.C. & Levin, S.A. (2012) Evolution of human-driven fire regimes in Africa. *Proceedings*
491 *of the National Academy of Sciences*, **109**, 847–852.
- 492 Benali, A., Mota, B., Carvalhais, N., Oom, D., Miller, L.M., Campagnolo, M.L. & Pereira, J.M.C. (2017)
493 Bimodal fire regimes unveil a global-scale anthropogenic fingerprint. *Global Ecology and Biogeography*,
494 **26**, 799–811.
- 495 Bird, R.B., Bird, D.W. & Coddling, B.F. (2016) People, El Niño southern oscillation and fire in Australia: fire
496 regimes and climate controls in hummock grasslands. *Philosophical transactions of the Royal Society of*
497 *London. Series B, Biological sciences*, **371**, 20150343.
- 498 Bird, R.B., Coddling, B.F., Kauhainen, P.G. & Bird, D.W. (2012) Aboriginal hunting buffers climate-driven fire-
499 size variability in Australia’s spinifex grasslands. *Proceedings of the National Academy of Sciences of the*
500 *United States of America*, **109**, 10287–10292.
- 501 Bistinas, I., Harrison, S.P., Prentice, I.C. & Pereira, J.M.C. (2014) Causal relationships versus emergent patterns
502 in the global controls of fire frequency. *Biogeosciences*, **11**, 5087–5101.
- 503 Bistinas, I., Oom, D., Sá, A.C.L., Harrison, S.P., Prentice, I.C. & Pereira, J.M.C. (2013) Relationships between
504 Human Population Density and Burned Area at Continental and Global Scales. *PLoS ONE*, **8**, e81188.

- 505 Boer, M.M., Bowman, D.M.J.S., Murphy, B.P., Cary, G.J., Cochrane, M.A., Fensham, R.J., Krawchuk, M.A.,
506 Price, O.F., De Dios, V.R., Williams, R.J. & Bradstock, R.A. (2016) Future changes in climatic water
507 balance determine potential for transformational shifts in Australian fire regimes. *Environmental Research*
508 *Letters*, **11**, 065002.
- 509 Bond, W.J., Woodward, F.I. & Midgley, G.F. (2005) The global distribution of ecosystems in a world without
510 fire. *New Phytologist*, **165**, 525–538.
- 511 Bowman, D.M.J.S., Balch, J., Artaxo, P., Bond, W.J., Cochrane, M.A., D’Antonio, C.M., DeFries, R., Johnston,
512 F.H., Keeley, J.E., Krawchuk, M.A., Kull, C.A., Mack, M., Moritz, M.A., Pyne, S., Roos, C.I., Scott, A.C.,
513 Sodhi, N.S. & Swetnam, T.W. (2011) The human dimension of fire regimes on Earth. *Journal of*
514 *Biogeography*, **38**, 2223–2236.
- 515 Bowman, D.M.J.S., Murphy, B.P., Williamson, G.J. & Cochrane, M.A. (2014) Pyrogeographic models,
516 feedbacks and the future of global fire regimes. *Global Ecology and Biogeography*, **23**, 821–824.
- 517 Bradstock, R.A. (2010) A biogeographic model of fire regimes in Australia: current and future implications.
518 *Global Ecology and Biogeography*, **19**, 145–158.
- 519 Burnham, K.P. & Anderson, D.R. (2004) Multimodel Inference Understanding AIC and BIC in Model Selection.
520 *Sociological Methods & Research*, **33**, 261–304.
- 521 Chen, Y., Morton, D.C., Andela, N., van der Werf, G.R., Giglio, L. & Randerson, J.T. (2017) A pan-tropical
522 cascade of fire driven by El Niño/Southern Oscillation. *Nature Climate Change*, **7**, 906–911.
- 523 Chen, Y., Randerson, J., Morton, D., DeFries, R., Collatz, G., Kasibhatla, P., Giglio, L., Jin, Y. & Marlier, M.
524 (2011) Forecasting fire season severity in South America using sea surface temperature anomalies.
525 *Science*, **334**, 787–791.
- 526 Chuvieco, E., Giglio, L. & Justice, C. (2008) Global characterization of fire activity: toward defining fire
527 regimes from Earth observation data. *Global Change Biology*, **14**, 1488–1502.
- 528 Cochrane, M.A. & Ryan, K.C. (2009) *Fire and fire ecology: Concepts and principles*. Springer Praxis Books.,
529 pp. 25–62. Springer Berlin Heidelberg.
- 530 Daniau, A.-L., Bartlein, P.J., Harrison, S.P., Prentice, I.C., Brewer, S., Friedlingstein, P., Harrison-Prentice, T.I.,
531 Inoue, J., Izumi, K., Marlon, J.R., Mooney, S., Power, M.J., Stevenson, J., Tinner, W., Andrič, M.,
532 Atanassova, J., Behling, H., Black, M., Blarquez, O., Brown, K.J., Carcaillet, C., Colhoun, E.A.,
533 Colombaroli, D., Davis, B.A.S., D’Costa, D., Dodson, J., Dupont, L., Eshetu, Z., Gavin, D.G., Genries, A.,
534 Haberle, S., Hallett, D.J., Hope, G., Horn, S.P., Kassa, T.G., Katamura, F., Kennedy, L.M., Kershaw, P.,
535 Krivonogov, S., Long, C., Magri, D., Marinova, E., McKenzie, G.M., Moreno, P.I., Moss, P., Neumann,
536 F.H., Norström, E., Paitre, C., Rius, D., Roberts, N., Robinson, G.S., Sasaki, N., Scott, L., Takahara, H.,
537 Terwilliger, V., Thevenon, F., Turner, R., Valsecchi, V.G., Vannièrè, B., Walsh, M., Williams, N. &
538 Zhang, Y. (2012) Predictability of biomass burning in response to climate changes. *Global*
539 *Biogeochemical Cycles*, **26**, GB4007.
- 540 DiMiceli, C.M., Carroll, M.L., Sohlberg, R.A., Huang, C., Hansen, M.C. & Townshend, J.R.G. (2011) *Annual*
541 *Global Automated MODIS Vegetation Continuous Fields (MOD44B) at 250 m Spatial Resolution for Data*
542 *Years Beginning Day 65, 2000 - 2010, Collection 5 Percent Tree Cover*, University of Maryland, College
543 Park, MD, USA.
- 544 Forkel, M., Dorigo, W., Lasslop, G., Teubner, I., Chuvieco, E. & Thonicke, K. (2017) A data-driven approach to
545 identify controls on global fire activity from satellite and climate observations (SOFIA V1). *Geoscientific*
546 *Model Development*, **10**, 4443–4476.
- 547 Friedl, M.A., Sulla-Menashe, D., Tan, B., Schneider, A., Ramankutty, N., Sibley, A. & Huang, X. (2010)
548 MODIS Collection 5 global land cover: Algorithm refinements and characterization of new datasets.
549 *Remote Sensing of Environment*, **114**, 168–182.
- 550 Funk, C., Peterson, P., Landsfeld, M., Pedreros, D., Verdin, J., Shukla, S., Husak, G., Rowland, J., Harrison, L.,
551 Hoell, A. & Michaelsen, J. (2015) The climate hazards infrared precipitation with stations—a new
552 environmental record for monitoring extremes. *Scientific Data*, **2**, 150066.
- 553 Giglio, L., Boschetti, L., Roy, D.P., Humber, M.L. & Justice, C.O. (2018) The Collection 6 MODIS burned area
554 mapping algorithm and product. *Remote Sensing of Environment*, **217**, 72–85.

- 555 Hantson, S., Arneth, A., Harrison, S.P., Kelley, D.I., Prentice, I.C., Rabin, S.S., Archibald, S., Mouillot, F.,
556 Arnold, S.R., Artaxo, P., Bachelet, D., Ciais, P., Forrest, M., Friedlingstein, P., Hickler, T., Kaplan, J.O.,
557 Kloster, S., Knorr, W., Lasslop, G., Li, F., Mangeon, S., Melton, J.R., Meyn, A., Sitch, S., Spessa, A., van
558 der Werf, G.R., Voulgarakis, A. & Yue, C. (2016) The status and challenge of global fire modelling. *13*,
559 3359–3375.
- 560 Hantson, S., Scheffer, M., Pueyo, S., Xu, C., Lasslop, G., van Nes, E.H., Holmgren, M. & Mendelsohn, J. (2017)
561 Rare, Intense, Big fires dominate the global tropics under drier conditions. *Scientific Reports*, **7**, 14374.
- 562 Hoffmann, W.A., Geiger, E.L., Gotsch, S.G., Rossatto, D.R., Silva, L.C.R., Lau, O.L., Haridasan, M. & Franco,
563 A.C. (2012) Ecological thresholds at the savanna-forest boundary: how plant traits, resources and fire
564 govern the distribution of tropical biomes. *Ecology Letters*, **15**, 759–768.
- 565 Hulme, M. & Viner, D. (1998) *A Climate Change Scenario for the Tropics. Potential Impacts of Climate Change*
566 *on Tropical Forest Ecosystems*, pp. 5–36. Springer Netherlands, Dordrecht.
- 567 Jolly, W.M., Cochrane, M.A., Freeborn, P.H., Holden, Z.A., Brown, T.J., Williamson, G.J. & Bowman, D.M.J.S.
568 (2015) Climate-induced variations in global wildfire danger from 1979 to 2013. *Nature Communications*,
569 **6**, 7537.
- 570 Kahiu, M.N. & Hanan, N.P. (2018) Fire in sub-Saharan Africa: The fuel, cure and connectivity hypothesis.
571 *Global Ecology and Biogeography*, **27**, 946–957.
- 572 Krawchuk, M.A. & Moritz, M.A. (2011) Constraints on global fire activity vary across a resource gradient.
573 *Ecology*, **92**, 121–132.
- 574 Lasslop, G., Moeller, T., D'Onofrio, D., Hantson, S. & Kloster, S. (2018) Tropical climate–
575 vegetation–fire relationships: multivariate evaluation of the land surface model JSBACH. *Biogeosciences*,
576 **15**, 5969–5989.
- 577 Lehmann, C.E., Anderson, T.M., Sankaran, M., Higgins, S.I., Archibald, S., Hoffmann, W.A., Hanan, N.P.,
578 Williams, R.J., Fensham, R.J., Felfili, J. & others (2014) Savanna vegetation-fire-climate relationships
579 differ among continents. *Science*, **343**, 548–552.
- 580 Lehmann, C.E.R., Archibald, S.A., Hoffmann, W.A. & Bond, W.J. (2011) Deciphering the distribution of the
581 savanna biome. *New Phytologist*, **191**, 197–209.
- 582 Lehsten, V., Harmand, P., Palumbo, I. & Arneth, A. (2010) Modelling burned area in Africa. *Biogeosciences*, **7**,
583 3199–3214.
- 584 van Marle, M.J.E., Kloster, S., Magi, B.I., Marlon, J.R., Daniau, A.-L., Field, R.D., Arneth, A., Forrest, M.,
585 Hantson, S., Kehrwald, N.M., Knorr, W., Lasslop, G., Li, F., Mangeon, S., Yue, C., Kaiser, J.W. & van der
586 Werf, G.R. (2017) Historic global biomass burning emissions based on merging satellite observations with
587 proxies and fire models (1750–2015). *Geoscientific Model Development Discussions*, **10**,
588 3329–3357.
- 589 Mataveli, G.A.V., Silva, M.E.S., Pereira, G., Cardozo, F.D.S., Kawakubo, F.S., Bertani, G., Costa, J.C., Ramos,
590 R.D.C. & Silva, V.V. Da (2018) Satellite observations for describing fire patterns and climate-related fire
591 drivers in the Brazilian savannas. *Hazards Earth Syst. Sci*, **18**, 125–144.
- 592 Mistry, J. (2000) *World savannas: ecology and human use*, Prentice Hall (a Pearson Education Company).
- 593 Moritz, M.A., Parisien, M.-A., Batllori, E., Krawchuk, M.A., Van Dorn, J., Ganz, D.J. & Hayhoe, K. (2012)
594 Climate change and disruptions to global fire activity. *Ecosphere*, **3**, 1–22.
- 595 Morton, D.C., DeFries, R.S., Nagol, J., Souza, C.M., Kasichke, E.S., Hurtt, G.C. & Dubayah, R. (2011)
596 Mapping canopy damage from understory fires in Amazon forests using annual time series of Landsat and
597 MODIS data. *Remote Sensing of Environment*, **115**, 1706–1720.
- 598 O'Donnell, A.J., Boer, M.M., McCaw, W.L. & Grierson, P.F. (2011) Vegetation and landscape connectivity
599 control wildfire intervals in unmanaged semi-arid shrublands and woodlands in Australia. *Journal of*
600 *Biogeography*, **38**, 112–124.
- 601 Le Page, Y., Oom, D., Silva, J.M.N., Jönsson, P. & Pereira, J.M.C. (2010) Seasonality of vegetation fires as
602 modified by human action: observing the deviation from eco-climatic fire regimes. *Global Ecology and*
603 *Biogeography*, **19**, 575–588.

- 604 Pausas, J.G. & Paula, S. (2012) Fuel shapes the fire–climate relationship: evidence from Mediterranean
605 ecosystems. *Global Ecology and Biogeography*, **21**, 1074–1082.
- 606 Pausas, J.G. & Ribeiro, E. (2013) The global fire–productivity relationship. *Global Ecology and Biogeography*,
607 **22**, 728–736.
- 608 Price, O.F., Pausas, J.G., Govender, N., Flannigan, M., Fernandes, P.M., Brooks, M.L. & Bird, R.B. (2015)
609 Global patterns in fire leverage: The response of annual area burnt to previous fire. *International Journal*
610 *of Wildland Fire*, **24**, 297–306.
- 611 Price, O.F., Russell-Smith, J. & Watt, F. (2012) The influence of prescribed fire on the extent of wildfire in
612 savanna landscapes of western Arnhem Land, Australia. *International Journal of Wildland Fire*, **21**, 297–
613 305.
- 614 R Core Team (2016) R: A language and environment for statistical computing. R Foundation for Statistical
615 Computing.
- 616 Rabin, S.S., Melton, J.R., Lasslop, G., Bachelet, D., Forrest, M., Hantson, S., Kaplan, J.O., Li, F., Mangeon, S.,
617 Ward, D.S., Yue, C., Arora, V.K., Hickler, T., Kloster, S., Knorr, W., Nieradzik, L., Spessa, A., Folberth,
618 G.A., Sheehan, T., Voulgarakis, A., Kelley, D.I., Prentice, I.C., Sitch, S., Harrison, S. & Arneeth, A. (2017)
619 The Fire Modeling Intercomparison Project (FireMIP), phase 1: experimental and analytical protocols with
620 detailed model descriptions. *Geoscientific Model Development*, **10**, 1175–1197.
- 621 Ratnam, J., Tomlinson, K.W., Rasquinha, D.N. & Sankaran, M. (2016) Savannahs of Asia: antiquity,
622 biogeography, and an uncertain future. *Philosophical transactions of the Royal Society of London. Series*
623 *B, Biological sciences*, **371**, 20150305.
- 624 Saha, M. V., Scanlon, T.M. & D’Odorico, P. (2019) Climate seasonality as an essential predictor of global fire
625 activity. *Global Ecology and Biogeography*, **28**, 198–210.
- 626 Voulgarakis, A. & Field, R.D. (2015) Fire Influences on Atmospheric Composition, Air Quality and Climate.
627 *Current Pollution Reports*, **1**, 70–81.
- 628 WCS, W.C.S.- & University, C. for I.E.S.I.N.-C.-C. (2005) Last of the Wild Project, Version 2, 2005 (LWP-2):
629 Global Human Influence Index (HII) Dataset (Geographic).
- 630 van der Werf, G.R., Randerson, J.T., Giglio, L., Gobron, N. & Dolman, A.J. (2008) Climate controls on the
631 variability of fires in the tropics and subtropics. *Global Biogeochemical Cycles*, **22**, GB3028.
- 632 Whitlock, C., Higuera, P.E., McWethy, D.B. & Briles, C.E. (2010) Paleocological perspectives on fire ecology:
633 revisiting the fire-regime concept. *Open Ecology Journal*, **3**, 6–23.
- 634 Van Wilgen, B.W., Govender, N., Biggs, H.C., Ntsala, D. & Funda, X.N. (2004) Response of Savanna Fire
635 Regimes to Changing Fire-Management Policies in a Large African National Park. *Conservation Biology*,
636 **18**, 1533–1540.
- 637 Williams, A.P. & Abatzoglou, J.T. (2016) Recent Advances and Remaining Uncertainties in Resolving Past and
638 Future Climate Effects on Global Fire Activity. *Current Climate Change Reports*, **2**, 1–14.
- 639 Yibarbuk, D., Whitehead, P.J., Russell-Smith, J., Jackson, D., Godjuwa, C., Fisher, A., Cooke, P., Choquenot, D.
640 & Bowman, D.M.J.S. (2002) Fire ecology and Aboriginal land management in central Arnhem Land,
641 northern Australia: a tradition of ecosystem management. *Journal of Biogeography*, **28**, 325–343.

642

643 **Data Accessibility:**

644 Biome wide gridded raster layers (GeoTIFF) of mean annual rainfall, tree cover, dry season duration,
645 and human development index, as well as per fire-year burned area and antecedent rainfall (6 and 24-
646 month accumulation periods) along with inferred maps of fire-response to antecedent rainfall are
647 available on Zenodo web site (<https://zenodo.org/>)

Tables

649 **Table 1.** Multiple Linear Regression Models explaining the variation of annual burned area
 650 anomalies ($BA_{i,j}$ anomaly) in pixel i and year j for tropical savannas and grasslands areas
 651 (2002 – 2016). The variables representing the fuel moisture effect (6 months of accumulated
 652 rainfall; $Rain6_{i,j}$), and the fuel build-up effect (24 months of accumulated rainfall; $Rain24_{i,j}$),
 653 varied both by pixel i and year j . Other variables, including mean annual rainfall (MAR_i), dry
 654 season duration (DS_i), human influence index (HII_i) and tree cover (TC_i) varied by pixel i
 655 only. Model performance was evaluated based on the coefficient of determination (R^2), p-
 656 value and Akaike's Information Criterion (AIC). All models were significant at $p < 0.001$.

<i>Regression model</i>	<i>Regression equation</i>	R^2	AIC
$Rain6_{i,j} + Rain24_{i,j}$	$BA_{i,j}$ anomaly $\sim -0.22 - 0.0018 * Rain6_{i,j} + 0.00040 * Rain24_{i,j} + \epsilon_{ij}$	0.0019	2090280
$Rain6_{i,j} : MAR_i + Rain24_{i,j} : MAR_i$	$BA_{i,j}$ anomaly $\sim 0.0098 - 0.0000011 * Rain6_{i,j} : MAR_i + 0.00000018 * Rain24_{i,j} : MAR_i + \epsilon_{ij}$	0.0013	2090422
$Rain6_{i,j} : Continent_i + Rain24_{i,j} : Continent_i$	$BA_{i,j}$ anomaly $\sim -0.43 - 0.0011 * Rain6_{i,j} : Africa_i - 0.0037 * Rain6_{i,j} : Australia_i - 0.0033 * Rain6_{i,j} : SouthAmerica_i + 0.00041 * Rain24_{i,j} : Africa_i + 0.00088 * Rain24_{i,j} : Australia_i + 0.00058 * Rain24_{i,j} : SouthAmerica_i + \epsilon_{ij}$	0.0029	2089998
$Rain6_{i,j} : Continent_i + Rain24_{i,j} : Continent_i + DS_i : Continent$	$BA_{i,j}$ anomaly $\sim 0.38 - 0.0012 * Rain6_{i,j} : Africa_i - 0.0034 * Rain6_{i,j} : Australia_i - 0.0035 * Rain6_{i,j} : SouthAmerica_i + 0.00023 * Rain24_{i,j} : Africa_i + 0.0014 * Rain24_{i,j} : Australia_i + 0.00051 * Rain24_{i,j} : SouthAmerica_i - 0.062 * DS_i : Africa_i - 0.31 * DS_i : Australia_i - 0.12 * DS_i : SouthAmerica_i + \epsilon_{ij}$	0.0034	2089875
$Rain6_{i,j} : Continent_i + Rain24_{i,j} : Continent_i + HII_i : Continent_i$	$BA_{i,j}$ anomaly $\sim -0.55 - 0.0011 * Rain6_{i,j} : Africa_i - 0.0036 * Rain6_{i,j} : Australia_i - 0.0033 * Rain6_{i,j} : SouthAmerica_i + 0.00040 * Rain24_{i,j} : Africa_i + 0.0011 * Rain24_{i,j} : Australia_i + 0.00054 * Rain24_{i,j} : SouthAmerica_i + 0.011 * HII_i : Africa_i - 0.11 * HII_i : Australia_i + 0.017 * HII_i : SouthAmerica_i + \epsilon_{ij}$	0.0031	2089957
$Rain6_{i,j} : Continent_i + Rain24_{i,j} : Continent_i + TC_i : Continent_i$	$BA_{i,j}$ anomaly $\sim -0.42 - 0.0012 * Rain6_{i,j} : Africa_i - 0.0038 * Rain6_{i,j} : Australia_i - 0.0033 * Rain6_{i,j} : SouthAmerica_i + 0.00049 * Rain24_{i,j} : Africa_i + 0.0015 * Rain24_{i,j} : Australia_i + 0.00050 * Rain24_{i,j} : SouthAmerica_i - 0.010 * TC_i : Africa_i - 0.13 * TC_i : Australia_i + 0.010 * TC_i : SouthAmerica_i + \epsilon_{ij}$	0.0034	2089868
$Rain6_{i,j} : Continent_i + Rain24_{i,j} : Continent_i + TC_i : Continent_i + DS_i : Continent_i + HII_i : Continent_i$	$BA_{i,j}$ anomaly $\sim 0.36 - 0.0012 * Rain6_{i,j} : Africa_i - 0.0036 * Rain6_{i,j} : Australia_i - 0.0036 * Rain6_{i,j} : SouthAmerica_i + 0.00035 * Rain24_{i,j} : Africa_i + 0.0019 * Rain24_{i,j} : Australia_i + 0.00046 * Rain24_{i,j} : SouthAmerica_i - 0.013 * TC_i : Africa_i - 0.13 * TC_i : Australia_i + 0.0077 * TC_i : SouthAmerica_i - 0.055 * DS_i : Africa_i - 0.29 * DS_i : Australia_i - 0.16 * DS_i : SouthAmerica_i - 0.0064 * HII_i : Africa_i + 0.058 * HII_i : Australia_i + 0.016 * HII_i : SouthAmerica_i + \epsilon_{ij}$	0.0039	2089756

657

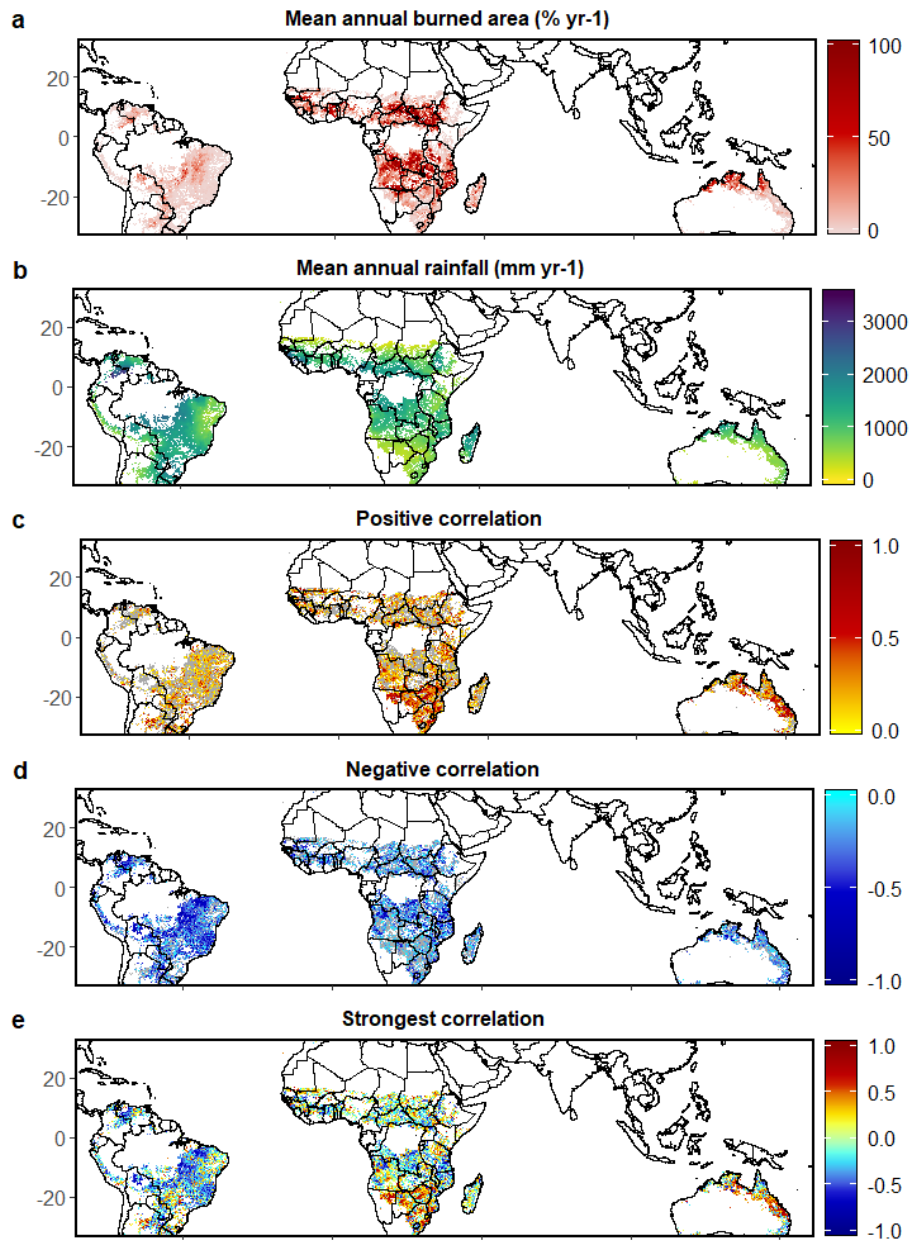
658

659

660

661
662

Figures



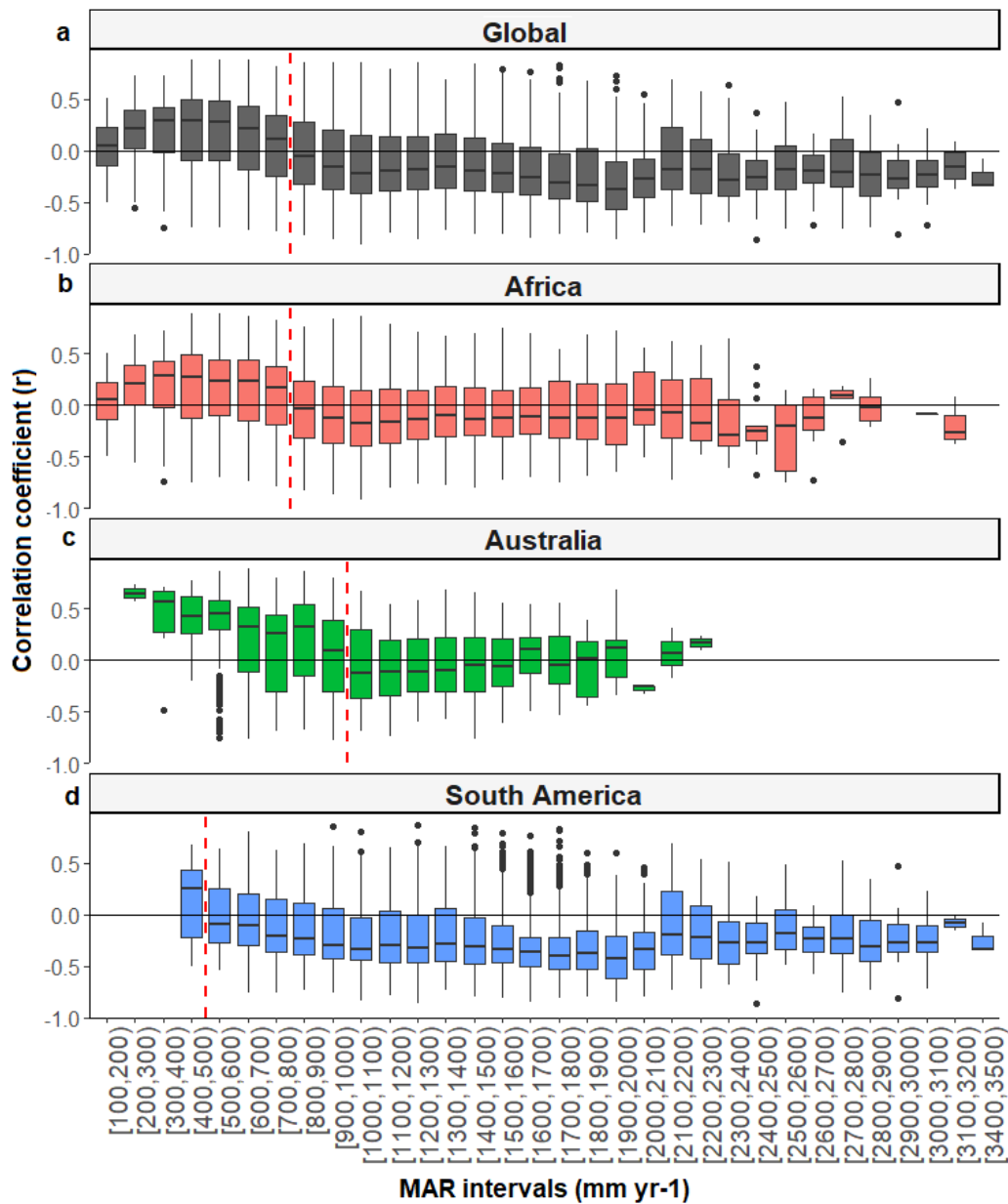
663
664

665 **Fig. 1.** Rainfall – burned area interactions varied widely across continents. (a) Mean annual
666 burned area ($\% \text{ yr}^{-1}$), (b) mean annual rainfall (mm yr^{-1}), (c) correlation between annual
667 burned area and 24 months of antecedent rainfall (positive correlations), (d) correlation
668 between annual burned area and 6 months of antecedent rainfall (negative correlations), and
669 (e) the strongest absolute correlation shown in (c and d). Figure e shows the distribution of
670 *fuel build-up limited* (positive correlation) and *fuel moisture limited* (negative correlation) fire
671 regimes across tropical savannas. Grid cells with land cover classes other than savannas and
672 grasslands were excluded from our analysis and are masked in white. Pixels with negative
673 correlations in b and positive correlations in c were masked in grey.

674

675

676



677

678

679

680

681

682

683

684

685

686

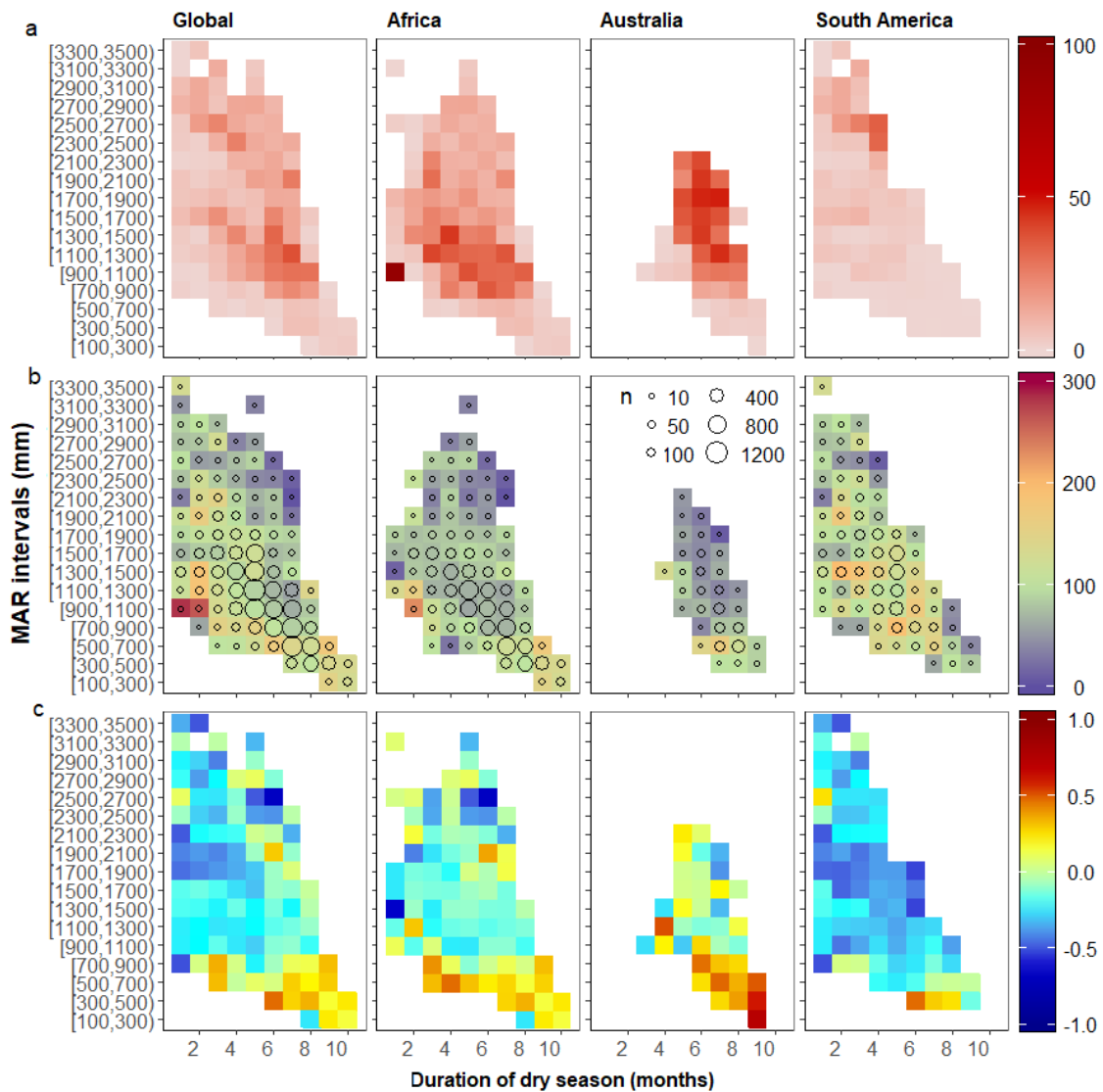
687

688

Fig. 2. Box-and-whisker plots of the response of burned area to antecedent rainfall. Results for (a) Pantropical savannas and grasslands, and for (b) Africa, (c) Australia, and (d) South America, separately. Box plots include all 0.25° grid cells per bin of 100 mm mean annual rainfall (MAR). For each grid cell we registered a single response (positive, based on 24-months of antecedent precipitation) or negative (based on 6 months of antecedent rainfall) using the per-grid cell strongest absolute correlation. The boxes indicate the 25th and 75th percentile of the data, the mid band indicates the median, and the whiskers indicate the 5th and 95th percentiles. Box plots with less than 5 pixels were excluded from this figure.

687

688

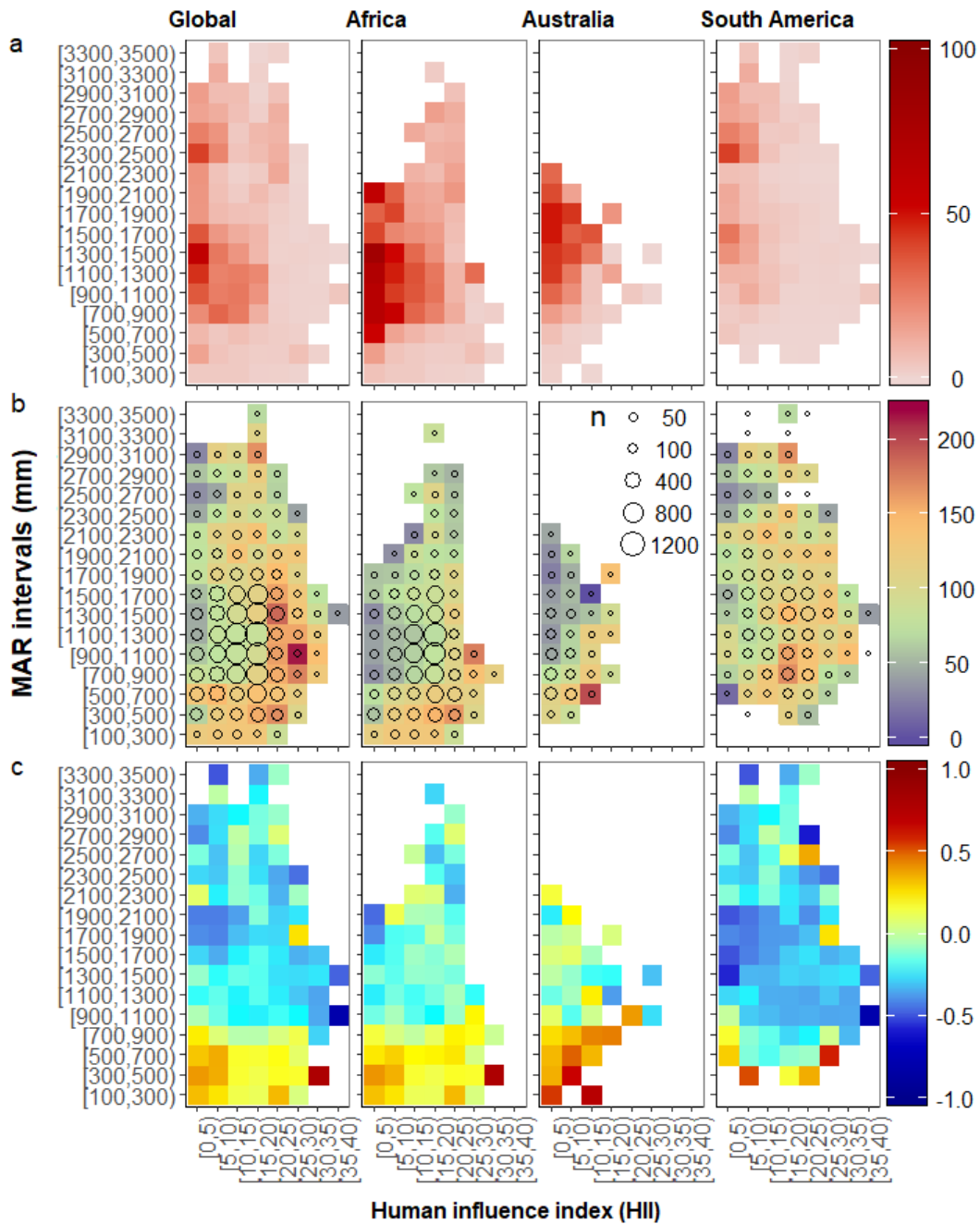


690

691 **Fig. 3.** Burned area response to dry season duration. (a) Median burned area (% yr⁻¹) per bin
 692 of Mean Annual Rainfall (MAR intervals) and dry season duration (b) Coefficient of variation
 693 of burned area per bin of Mean Annual Rainfall and dry season duration, circle size represent
 694 the upper limit of the number of grid cells by bin (n = number of grid cells). (c) Median
 695 correlation coefficient based on the per-pixel strongest absolute correlation within each bin of
 696 Mean Annual Rainfall and dry season duration. Cells with less than 3 pixels were excluded
 697 from panel b because the coefficients of variation calculate require at least 3 data.
 698

699

700



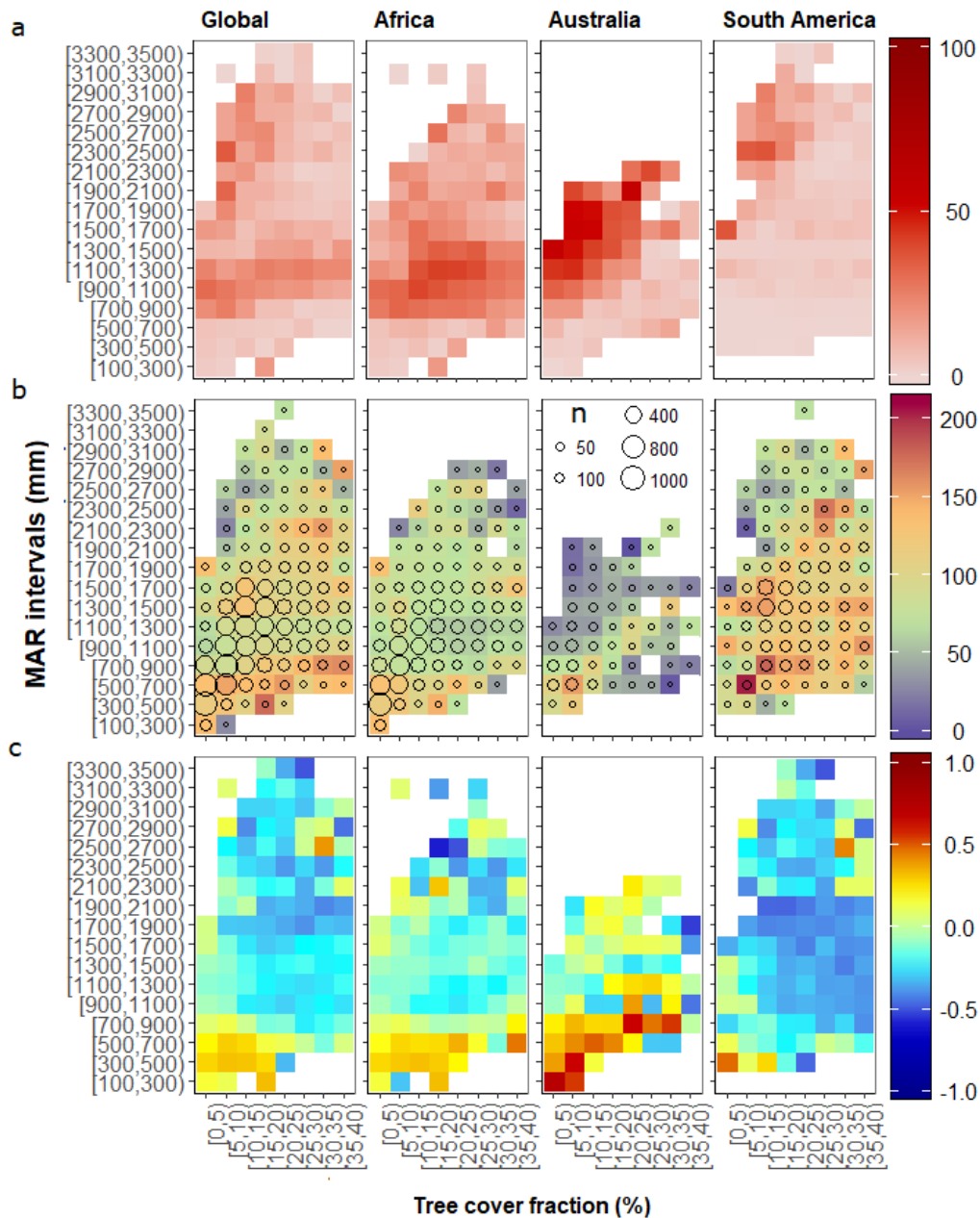
701

702 **Fig. 4.** Burned Area response to human land management. (a) Median burned area (% yr⁻¹)
 703 per bin of Mean Annual Rainfall (MAR intervals) and Human influence index. (b) Coefficient
 704 of variation of burned area per bin of Mean Annual Rainfall and Human influence index,
 705 circle size represent the upper limit of the number of grid cells by bin (n = number of grid
 706 cells). (c) Median correlation coefficient, based on the per-pixel strongest absolute correlation
 707 within each bin of Mean Annual Rainfall and Human influence index. Cells with less than 3
 708 pixels were excluded from panel b because the coefficients of variation calculate require at
 709 least 3 data.

710

711

712



715
716 **Fig. 5.** Burned Area response to tree cover fraction. (a) Median burned area (% yr⁻¹) per bin of
717 Mean Annual Rainfall (MAR intervals) and tree cover fraction (%). (b) Coefficient of
718 variation of burned area per bin of Mean Annual Rainfall and tree cover fraction, circle size
719 represent the upper limit of the number of grid cells by bin (n = number of grid cells). (c)
720 Median correlation coefficient, based on the per-pixel strongest absolute correlation within
721 each bin of Mean Annual Rainfall and tree cover fraction. Cells with less than 3 pixels were
722 excluded from panel b because the coefficients of variation calculate require at least 3 data.
723
724